pagepress

Journal of Agricultural Engineering

Journal of Agricultural Engineering 2026; LVII:1749
doi:10.4081/jae.2025.1749

©Copyright: the Author(s), 2025
Licensee PAGEPress, Italy

Monitoring water-stressed spring tea canopy temperature using UAV-derived indices and clustering models

Jiaxing Xie,[1,2] Yazhong Chen,[1] Shuai Zhao,[1] Jiaxin Wang,[1] Liye Chen,[1] Fan Luo,[1] Zihao Chen,[1] Weixian Sha,[1] Peng Gao,[1] Weixing Wang,[3] Hongshan Liu[1,2]

[1]College of Electronic Engineering (College of Artificial Intelligence), South China Agricultural University, Guangzhou; [2]Engineering Research Center for Monitoring Agricultural information of Guangdong Province, Guangzhou; [3]Zhujiang College, South China Agricultural University, Guangzhou, China

Abstract

This study developed a rapid method for monitoring water stress in tea trees using unmanned aerial vehicle (UAV) multispectral imaging combined with machine learning models. The study analyzed tea trees subjected to five different irrigation treatments. UAV multispectral imaging and ground-based measurements were employed to explore the relationships between canopy-air temperature differences, soil moisture content, spectral reflectance, vegetation indices, and canopy temperature. The ordering points to identify the clustering structure (OPTICS) algorithm was used to cluster soil moisture content and canopy-air temperature difference data. The clustering process determined the radius parameter (ϵ) from an ordered decision graph, establishing the upper and lower limits of the canopy-air temperature difference. These limits were then correlated with the vapor pressure deficit (VPD) lower limit equation for fully irrigated tea trees to validate the effectiveness of the OPTICS algorithm. Several machine learning regression models, including random forest (RF), support vector regression (SVR), K-nearest neighbors (KNR), and backpropagation (BP) neural networks, were used to create an inversion model for predicting canopy temperature based on vegetation indices. A strong correlation (coefficient of 0.74) was observed between the canopy-air temperature difference bounds derived from OPTICS clustering and the crop water stress index (CWSI) values calculated from empirical model data. Spectral reflectance at 450 nm, 560 nm, and 650 nm remained stable, while reflectance at 730 nm and 840 nm increased significantly with rising canopy temperature. The RF model demonstrated robust performance, achieving an R^2 value greater than 0.8, and effectively predicted canopy temperature using vegetation indices. By combining density-based OPTICS clustering to establish water stress index limits and leveraging vegetation indices for canopy temperature inversion, this study presents a rapid and accurate method for calculating the water stress index in tea trees. The findings provide a foundation for UAV-based remote sensing applications in monitoring tea tree water stress and highlight potential advancements in precision irrigation management.

Key words: Tea tree; canopy temperature; water stress index; UAV remote sensing; multispectral; machine learning.

Correspondence: Hongshan Liu, College of Electronic Engineering (College of Artificial Intelligence), South China Agricultural University, Guangzhou 510642, China. E-mail: hugouliu@scau.edu.cn

Introduction

Tea trees require substantial water for growth and development (Li *et al*., 2021; Kumar Jha *et al*., 2019; Wang *et al*., 2021). Adequate water supply and relative humidity significantly enhance tea quality and yield, whereas insufficient water or low humidity often result in coarse, low-quality leaves, ultimately reducing the economic benefits of the tea industry (Huang *et al*., 2019; Yubin *et al*., 2019; Zou *et al*., 2023). In addition to water availability, tea trees are highly sensitive to temperature, with physiological processes regulated by minimum, optimal, and maximum temperature threshold (Awais *et al*., 2023; Maimaitijiang *et al*., 2020; Yin *et al*., 2019). When subjected to water stress, tea trees experience stomatal closure, reduced transpiration, and increased canopy temperature, making canopy temperature a critical indicator of water stress (Harle *et al*., 2024; Maes and Steppe, 2019; Shi *et al*., 2022; Wu and Mao, 2022). Monitoring water stress during the spring tea harvest is especially crucial due to its impact on the quality, yield, and market value of tea (Liu *et al*., 2021; Zou *et al*., 2023, 2023).

Current methods for quantifying water stress in tea trees primarily rely on determining the upper and lower baselines of the canopy-air temperature difference (de Castro *et al*., 2021; Harle *et al*., 2024; Idso *et al*., 1981). These baselines are essential for calculating the CWSI, a widely used parameter for assessing crop water stress (Kouadio *et al*., 2023; Li *et al*., 2021; Zhang *et al*., 2021). However, these baselines are highly sensitive to meteorological factors such as air temperature, relative humidity, and solar radiation, which can fluctuate rapidly. This variability complicates

the accurate and stable determination of CWSI, limiting its reliability for precision irrigation (Bhandari *et al*., 2018; Harle *et al*., 2024, 2024). Machine learning models have been explored to predict CWSI baselines based on meteorological data, but their generalizability is often constrained by the dynamic variability of environmental conditions (Ge *et al*., 2019). Thus, a more robust and adaptable approach is needed to monitor tea tree water stress effectively. In recent years, UAV-based multispectral remote sensing has emerged as a powerful tool for efficient crop monitoring (Huang *et al*., 2019; Khanal *et al*., 2020; Maimaitijiang *et al*., 2020). UAVs enable the collection of high-resolution multispectral data, capturing spectral reflectance at different wavelengths to calculate vegetation indices that can infer crop growth parameters and physiological states (Deng *et al*., 2018; Wang *et al*., 2021; Zou *et al*., 2023). For instance, spectral data combined with models such as R and SVR have demonstrated success in predicting canopy temperature for crops like wheat and rice (Ge *et al*., 2019; Romero *et al*., 2018). However, applications of UAV multispectral imaging for tea trees remain limited, especially for long-term water stress monitoring (Guofeng *et al*., 2022; Maes and Steppe, 2019). Moreover, traditional CWSI models struggle to adapt to dynamic environmental conditions, further restricting their effectiveness in precision agriculture (Kouadio *et al*., 2023; Liu *et al*., 2021; Zou *et al*., 2023).

To overcome these challenges, this study introduces a novel approach that integrates UAV multispectral imaging, machine learning models, and the density-based OPTICS clustering algorithm for monitoring water stress in tea trees. Specifically, UAVs were employed to collect spectral reflectance data, which were used to calculate vegetation indices and predict canopy temperature. Machine learning models, including RF, SVR, KNR, and BP neural networks, were used to establish predictive models for canopy temperature. The OPTICS clustering algorithm was further applied to stabilize the upper and lower baselines of canopy-air temperature differences, addressing the limitations of traditional empirical models.

Compared to existing methods, this approach offers several advantages. UAV-based multispectral imaging allows for rapid and accurate data acquisition across large tea plantations, while machine learning provides robust predictive capabilities for canopy temperature estimation. Notably, traditional approaches for crop water stress index (CWSI) often rely on empirically derived or fixed baseline values for canopy-air temperature differences, which are highly sensitive to environmental variability (Kouadio *et al*., 2023). In contrast, this study introduces the OPTICS clustering algorithm to dynamically extract upper and lower CWSI bounds based on actual field conditions, including soil moisture and thermal data. This clustering-based approach enhances robustness and adaptability under heterogeneous microclimates.

Additionally, the OPTICS clustering algorithm effectively mitigates the impact of meteorological variability by establishing stable baselines for CWSI calculation. To the best of our knowledge, this is the first application of combining UAV-based vegetation indices with OPTICS clustering for real-time tea plantation water stress monitoring. Together, these innovations enhance the accuracy, scalability, and reliability of water stress monitoring in tea trees. By integrating these advanced technologies, this study proposes a comprehensive and scalable solution for monitoring tea tree water stress. The findings not only provide theoretical support for precision irrigation management but also address broader challenges in adapting crop water stress monitoring methods to dynamic environmental conditions. This approach lays the groundwork for advancing UAV-based remote sensing applications in agriculture and promoting sustainable tea production practices.

Materials and Methods

Study area

The study was conducted in a tea plantation at South China Agricultural University, Guangzhou, Guangdong Province, China (113°36′E, 23°15′N). This region experiences a subtropical monsoon climate characterized by warm, humid springs, an average annual temperature of approximately 22°C, and abundant rainfall, making it suitable for studying the physiological and ecological characteristics of tea trees. The soil in the study area is classified as red sandy soil (80% red soil, 20% sandy soil) with good drainage and aeration properties and a field capacity of 27%, providing an ideal substrate to investigate the effects of varying water treatments on tea tree canopy temperature and soil moisture.

The experiment, conducted from March to April 2023, utilized the Huanong No. 1 tea variety developed by South China Agricultural University. The experimental field was divided into five water treatment zones (T1-T5), each measuring 2 m × 0.5 m. The water treatments were designed to simulate conditions ranging from adequate irrigation to extreme drought, based on the drought tolerance of tea trees and practical irrigation requirements:
T1: Adequate irrigation (field capacity of 85-95%)
T2: Mild stress (field capacity of 75-85%)
T3: Moderate stress (field capacity of 55-65%)
T4: Severe stress (field capacity of 45-55%)
T5: No irrigation.

Data acquisition

Data were collected between March 1 and April 16, 2023, under clear, cloudless weather conditions to ensure the accuracy of both multispectral imagery and meteorological data. Meteorological data were recorded every 10 minutes, while soil moisture and canopy temperature data were measured before and after each UAV flight. The data collection process is illustrated in Figure 1.

UAV multi-spectral image acquisition

A DJI Phantom 4 Multispectral UAV was employed to capture images of the tea tree canopy across five spectral bands: blue, green, red, red-edge, and near-infrared. These bands encompass key wavelengths in the visible and near-infrared spectra, effectively representing tea tree growth conditions and water stress levels. The UAV operated at an altitude of 10 meters, with forward and side overlap rates set at 80%. Images were captured at a resolution of 1600 × 1300, ensuring high-quality coverage of the tea canopy for subsequent image stitching. To ensure precise radiometric calibration, reflectance values specific to the DJI Phantom 4 Multispectral camera were applied (blue: 25.095%, green: 26.648%, red: 26.687%, red-edge: 26.680%, near-infrared: 28.000%). These calibration values, derived from a standard reference panel, minimized atmospheric and sensor-related effects, ensuring accuracy in subsequent vegetation index calculations.

Ground data acquisition

Ground-based data collection included meteorological observations and measurements of physiological characteristics of tea trees.

OPEN ACCESS

Meteorological data: An intelligent video weather station was installed 1 meter above the tea canopy to collect real-time data on air temperature, humidity, light intensity, wind speed, wind direction, and rainfall. Measurements were recorded every 10 minutes, providing comprehensive 24-hour environmental information.

Canopy temperature: Canopy temperature was measured using a Raytek ST18 infrared thermometer with an accuracy of ±0.2°C. To minimize random errors, each leaf was measured three times, and the average value was calculated. Measurements were conducted from a distance of 30 cm to ensure precise focus of the infrared beam on the leaf surface. For each treatment group, 20 representative tea leaves were randomly selected for measurement. All measurements were performed between 10:30 and 12:00 a.m. on clear-sky days to minimize variability due to sun angle and ambient conditions. The sensor was oriented perpendicular to the leaf surface during measurement to reduce angular distortion and ensure consistency.

Soil moisture content: Soil volumetric moisture content was measured using a JK-300F soil moisture meter with an accuracy of ±0.2%. This device enabled rapid and reliable monitoring of soil water dynamics, making it suitable for the experimental conditions.

Multispectral image processing workflow

Multispectral image processing was conducted to ensure the accuracy and usability of data for vegetation index calculations. Initially, radiometric calibration was performed using DJI Terra software. A standard calibration panel was utilized to adjust reflectance values, ensuring consistency between the collected data and actual canopy reflectance. This step provided reliable input data for subsequent vegetation index computations. Following calibration, images captured during the UAV flight in five spectral bands were reconstructed and stitched together to generate complete multispectral image files (Guptha *et al*., 2021; Huang *et al*., 2019). The radiometric calibration was based on calibration panel images captured on the same day as the flight. The Phantom 4 Multispectral camera's reflectance panel was used, with preset reflectance values for each band: blue (25.095%), green (26.648%), red (26.687%), red-edge (26.680%), and near-infrared (28.000%). These values were entered into DJI Terra to correct for atmospheric interference. The software also completed orthorectification and georeferencing using embedded GPS data. A simplified version of the complete processing workflow is illustrated in Figure 2.

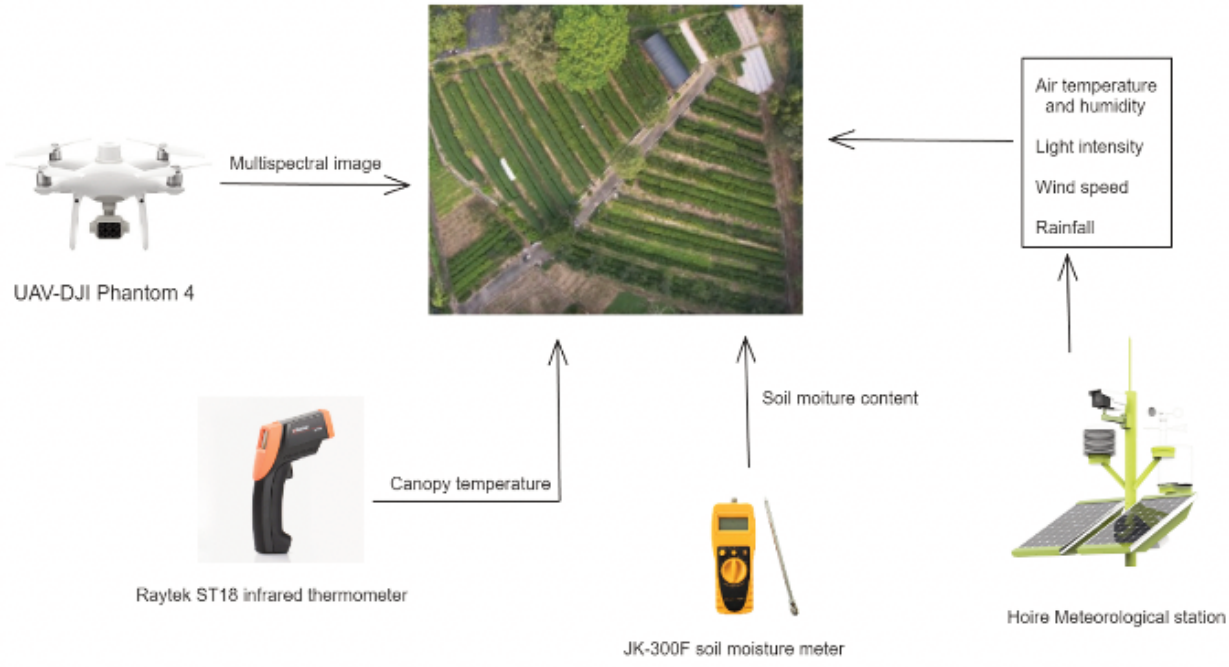

Figure 1. Data collection system and workflow for monitoring tea tree water stress.

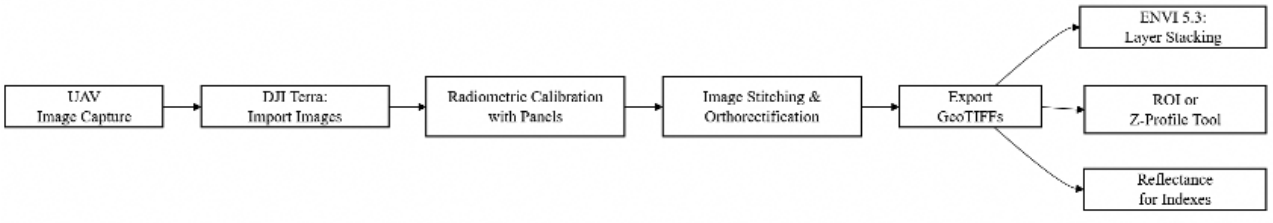

Figure 2. Workflow of UAV multispectral image processing: including radiometric calibration, orthomosaic generation using DJI Terra, and reflectance extraction and analysis in ENVI 5.3.

To further process the data, ENVI 5.3 software was employed. The Layer Stacking tool was used to merge raw images from the five spectral bands into a single multispectral image, ensuring proper spatial alignment across all bands. The ZProfile tool was then applied to extract spectral reflectance data from Regions of Interest (ROI), carefully selecting representative areas of the tea tree canopy while avoiding interference from shadows and weeds. This approach ensured the extraction of accurate and representative reflectance data. Based on the spectral reflectance data, vegetation indices were calculated to characterize the physiological conditions of the tea tree canopy. These indices, derived from spectral reflectance, are commonly used to infer vegetation health and stress levels. The following indices were selected for this study: normalized difference vegetation index (NDVI); renormalized difference vegetation index (RDVI); difference vegetation index (DVI); optimized soil-adjusted vegetation index (OSAVI).

These indices effectively reflect tea tree growth conditions and water stress levels. By analyzing the temporal trends of these vegetation indices and their correlation with canopy temperature, the water stress state of tea trees was predicted with higher accuracy. The specific formulas for calculating the vegetation indices are as follows:

$$NDVI = \frac{R_{NIR} - R_{RED}}{R_{NIR} + R_{RED}}$$
$$RDVI = \frac{R_{NIR} - R_{RED}}{\sqrt{(R_{NIR} + R_{RED})}}$$
$$DVI = R_{NIR} - R_{RED}$$
$$OSAVI = \frac{(1 + 0.16) \times ((R_{NIR} - R_{RED})}{(R_{NIR} + R_{RED} + 0.16} \quad \text{(Eq. 1)}$$

where R_{NIR} is the reflectance of the near-infrared band (840 nm); R_{RED} is the reflectance of the red band (650 nm).

Calculation method of CWSI of tea plant

The formula for calculating the CWSI is as follows:

$$CWSI = \frac{(T_c - T_a) - (T_c - T_a)_{II}}{(T_c - T_a)u_1 - (T_c - T_a)_{II}} \quad \text{(Eq. 2)}$$

where T_c is the tea tree canopy temperature (°C); T_a is the air temperature above the tea tree (°C); $(T_c - T_a)_{II}$ is the lower limit of the canopy-air temperature difference, which represents the canopy-air temperature difference when stomata are completely closed with no transpiration (°C); $(T_c - T_a)u_1$ is the upper limit of the canopy-air temperature difference, which represents the canopy-air temperature difference when stomata are fully open under full transpiration (°C).

The equations for the lower and upper limits are:

$$(T_c - T_a)_{II} = m \times VPD + C$$
$$VPD = 0.61078 \times e^{\frac{17.27 \times T_a}{T_a + 237.3}} \times (1 - RH)$$
$$(T_c - T_a)_{u_1} = m \times VPG + C$$
$$VPG = VPD(T_a) - VPD(T_a + C) \quad \text{(Eq. 3)}$$

where m and C are linear regression coefficients; is the air relative humidity in percentage; VPD is the vapor pressure deficit in Pa; VPG is the difference between the air saturation vapor pressure at temperature T_a and the air saturation vapor pressure at temperature $T_a + C$. The values of VPD and VPG are calculated using meteorological parameters T_a and RH.

OPTICS clustering algorithm

OPTICS is an enhanced density-based clustering algorithm that improves upon the traditional DBSCAN algorithm, particularly in handling noise points and irregularly shaped clusters (Ndlovu *et al*., 2021; Su *et al*., 2020; Wang *et al*., 2014). In this study, OPTICS was employed to classify soil moisture and canopy-air temperature difference data with greater precision, providing a more robust foundation for calculating the CWSI of tea trees.

As an extension of DBSCAN, OPTICS generates an ordered list of points and determines cluster categories based on an appropriate neighborhood radius (ϵ). This algorithm was applied to classify canopy-air temperature difference and soil moisture data, enabling the extraction of upper and lower boundaries for more accurate determination of the water stress state of tea trees. Compared to DBSCAN, OPTICS offers improved performance in managing noise and irregular cluster shapes by generating an ordered sequence and calculating reachability distances (Cheng *et al*., 2024; Feroz and Abu Dabous, 2021; Jeong *et al*., 2016). This capability allows for more precise identification of the relationship between soil moisture and canopy-air temperature differences, avoiding potential errors in traditional methods.

The OPTICS algorithm requires two main parameters: the minimum number of points (MinPts), which specifies the minimum number of samples required within the neighborhood radius, and the neighborhood radius (ϵ). Points that do not meet the MinPts requirement are considered noise points. In this experiment, MinPts was set to 9, and the clustering radius ϵ to 0.75.

The ordered sequence generated by OPTICS represents the processing order of data points. On a plot of the ordered sequence, the x-axis denotes the order of processing, while the y-axis represents the reachability distance. Mathematically, the ordered list can be expressed as {Pi} = {21,35,6…}, where the 21st node is processed first, followed by the 35th and 6th nodes.

The reachability distance determines whether one data point is accessible from another. If a point p can reach another point q *via* a series of intermediate points, p is considered reachable from q. This reachability is evaluated by comparing the reachability distance between p and q with MinPts. If the reachability distance is less than or equal to MinPts, the point is deemed reachable. By applying these principles, OPTICS facilitated the accurate classification of soil moisture and canopy-air temperature difference data in this study, providing the necessary boundaries for calculating the CWSI and improving the assessment of tea tree water stress.

Canopy temperature prediction model

This study utilized various regression models to predict the canopy temperature of tea plants, including BP neural networks, SVR, RF and KNR. Each model has distinct advantages and is suitable for specific scenarios, contributing to improved prediction accuracy and error reduction (Osco *et al*., 2021; Pipatsitee *et al*., 2023; Tsouros *et al*., 2019).

The BP neural network is widely applied in regression tasks. It consists of an input layer, hidden layers, and an output layer. The network's weights and biases are optimized through the backpropagation algorithm. During training, the network parameters are

OPEN ACCESS

iteratively adjusted until the predicted results converge with the target values or the loss function stabilizes. In this study, the mean squared error (MSE) was employed as the loss function to quantify the average difference between predicted and actual values.

The SVR model, a regression application of support vector machines (SVM), minimizes errors and enhances regression accuracy by maximizing the margin between samples and the decision surface. Random forest regression, an ensemble learning method, is well-suited for regression tasks. It aggregates predictions from multiple decision trees to produce the final output. Each decision tree is trained on a randomly selected subset of samples and features, and the final prediction is obtained by averaging the results of all decision trees. To prevent overfitting in this experiment, the minimum sample size for node splitting and leaf nodes was set to 5. KNR is an instance-based learning method that predicts a sample's value by averaging or weighting the values of its K nearest neighbors. In this study, Euclidean distance was used to measure the proximity of neighboring points, with K set to 6.

To evaluate the performance of these machine learning regression models, the following metrics were used:

- Coefficient of determination (R^2): measures the goodness of fit for the model.
- Root mean squared error (RMSE): quantifies the dispersion between predicted and actual values.
- Mean absolute error (MAE): represents the average difference between predicted and actual values.

The formulas for these metrics are as follows:

$$R^2 = 1 - \frac{\sum_i (\hat{y}_i - y_i)^2}{\sum_i (\bar{y}_i - y_i)^2}$$

$$RMSE = \sqrt{\frac{1}{m}\sum_{i=1}^{m}(y_i - \hat{y}_i)^2}$$

$$MAE = \frac{1}{m}\sum_{i=1}^{m}|(y_i - \hat{y}_i)|$$

These metrics provide a comprehensive assessment of the model's performance, facilitating comparisons between different approaches for canopy temperature prediction.

The selection of regression models -random forest (RF), support vector regression (SVR), K-nearest neighbors (KNR), and backpropagation (BP) neural networks- was based on their strong track record in agricultural remote sensing applications and their effectiveness in modeling complex, non-linear relationships. These models offer high interpretability, are computationally efficient, and have been successfully applied in canopy temperature estimation and crop stress monitoring (Ge *et al*., 2019; Osco *et al*., 2021; Romero *et al*., 2018). Although deep learning models such as convolutional neural network (CNN) and long short-term memory network (LSTM) have shown promise in large-scale agricultural studies, they are typically designed to process image sequences or time-series data. In this study, the input data (vegetation indices) are one-dimensional numerical features rather than raw image sequences or time-series data, which are more appropriate for CNN or LSTM architectures. Moreover, the primary goal of this study was to establish a lightweight, scalable, and interpretable framework for field-deployable canopy temperature estimation, which conventional ML models are better suited for.

Results

Determining canopy-air temperature bounds using OPTICS clustering

The canopy-air temperature difference represents the variation in temperature between the tea tree canopy and the surrounding air, serving as a critical indicator of water stress levels. Soil moisture content is closely linked to this temperature difference: when soil moisture is low, stomata close, transpiration decreases, and canopy temperature rises, resulting in a larger temperature difference. Conversely, when soil moisture is high, transpiration increases, leading to a lower canopy-air temperature difference. To determine the upper and lower bounds of the canopy-air temperature difference, this study applied the OPTICS clustering algorithm to analyze soil moisture and canopy-air temperature difference data collected from different moisture treatment zones (T1 to T5). Figure 3 presents the clustering results, illustrating the distribution of various data points. This figure illustrates the clustering results of soil moisture and canopy-air temperature difference data points, classified into three clusters (A, B, and C) using the OPTICS algorithm. Cluster A (blue squares) represents low soil moisture conditions, cluster B (green diamonds) represents medium soil moisture conditions, and cluster C (red triangles) corresponds to high soil moisture conditions. Grey points represent outliers that do not belong to any cluster. Figure 4

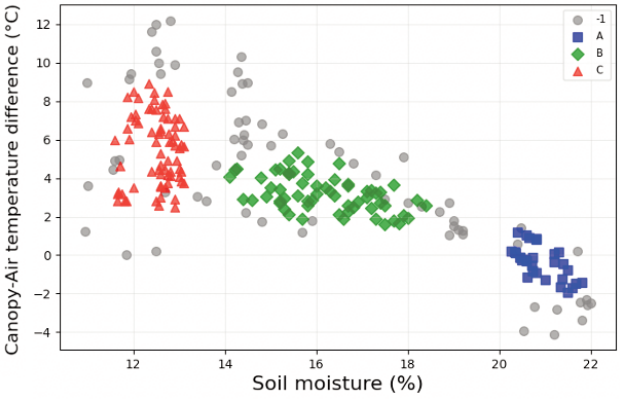

Figure 3. OPTICS clustering diagram for canopy-air temperature difference and soil moisture data.

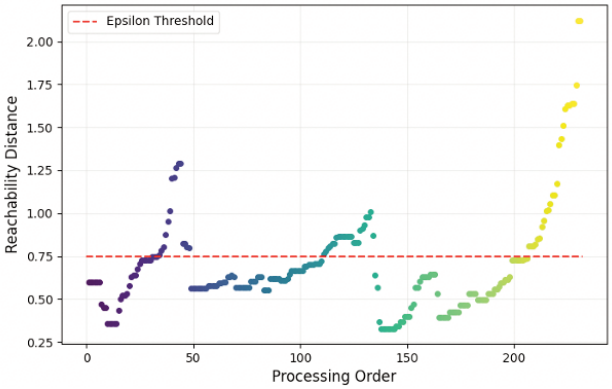

Figure 4. OPTICS ordered decision diagram for canopy-air temperature difference data.

depicts the OPTICS ordered decision diagram, which reveals the clustering characteristics of each data point. The red dashed line represents the epsilon threshold (ϵ= 0.75), which separates clusters. Data points below the threshold form distinct clusters, corresponding to low, medium, and high soil moisture conditions (clusters A, B, and C). Outliers are represented as isolated points above the threshold. From the analysis, the average canopy-air temperature difference for cluster C (representing high soil moisture) was calculated as -0.376°C, defining the lower bound. For cluster A (representing low soil moisture), the average canopy-air temperature difference was 5.52°C, defining the upper bound. These bounds were subsequently used in the calculation of the CWSI, providing a clear understanding of the physiological response of tea trees under varying moisture conditions.

The results from Figure 3, showing the OPTICS clustering diagram, illustrate the clustering distribution of data points across different moisture levels. Meanwhile, Figure 4, the ordered decision diagram, further validates the clustering results and supports the establishment of accurate CWSI bounds. The clear identification of upper and lower bounds not only simplifies the calculation of CWSI but also enhances its accuracy, thereby improving the assessment of tea tree water stress.

CWSI calculation and verification

CWSI is a critical parameter for evaluating water stress in tea trees. In this study, the CWSI was calculated using the method previously described, which combines the linear regression relationship between VP and the canopy-air temperature difference, along with the upper and lower bounds determined using the OPTICS clustering algorithm.

Under fully irrigated conditions, a linear regression model was developed to describe the relationship between VPD and the lower bound of the canopy-air temperature difference, yielding the following equation:

$$(T_c - T_a)_{II} = -2.118091 \times VPD + 3.374 \quad \text{(Eq. 4)}$$

The coefficient of determination (R^2=0.811) indicates a strong fit. Figure 5 illustrates this regression, highlighting a significant negative correlation between VPD and the lower bound of the canopy-air temperature difference, validating the use of VPD as a reliable water stress indicator. The upper and lower bounds derived from OPTICS clustering, combined with actual canopy temperature (T_C) data, were then applied to compute the CWSI under various moisture conditions. Figure 6 compares the measured and predicted CWSI values, demonstrating a strong linear correlation (R^2=0.74). Notably, the CWSI derived from OPTICS clustering provided more stable results, particularly for rapid assessments of water stress in tea trees under varying moisture conditions.

Canopy temperature and spectral reflectance analysis

Canopy temperature and spectral reflectance are critical indicators for assessing water stress in tea trees. Figure 7 illustrates the variation in canopy temperature under different water treatments. Under sufficient irrigation (T1), the canopy temperature remains relatively stable, with minimal fluctuations. However, as water stress intensifies (*e.g.*, T4 and T5), the fluctuation range of canopy temperature increases significantly, with the maximum temperature difference exceeding 10°C. This suggests that reduced transpiration and stomatal closure have a pronounced impact on the canopy temperature of tea trees.

Figure 8 depicts the variation in spectral reflectance across different moisture conditions. Under full irrigation (T1) and extreme water stress (T5), higher canopy temperatures are associated with a significant increase in reflectance in the red-edge (730 nm) and near-infrared (840 nm) bands. These changes are attributed to water stress-induced alterations in photosynthesis and transpiration, which affect the internal structure of leaves and their light absorption properties. In contrast, the reflectance in the blue (450 nm) and green (560 nm) bands exhibits minimal variation across treatments.

Table 1 summarizes the characteristics of vegetation indices under varying moisture conditions. In the T1 zone with adequate soil moisture, vegetation indices such as NDVI and NIR show low

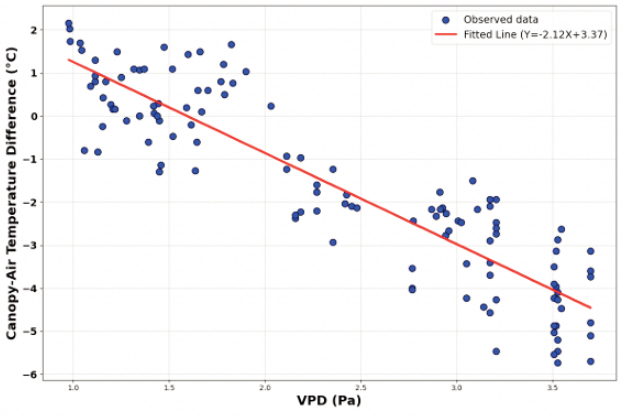

Figure 5. Linear regression relationship between VPD and the lower bound of the canopy-air temperature difference ($T_c - T_a$) under fully irrigated conditions. The fitted line (Y=−2.12X+3.37Y) demonstrates a strong negative correlation (R^2=0.811), confirming the importance of VPD as an indicator of water stress in tea trees.

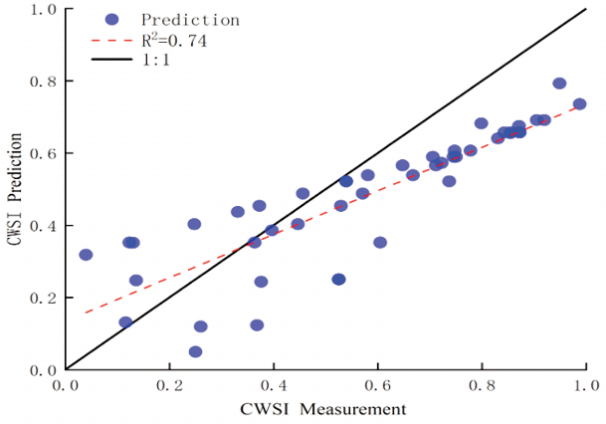

Figure 6. Comparison of measured and predicted CWSI values across various moisture conditions. The dashed red line represents the regression line (R^2=0.74), while the solid black line indicates the ideal 1:1 relationship. The strong linear correlation highlights the accuracy of the OPTICS clustering-based CWSI calculation method for assessing tea tree water stress.

OPEN ACCESS

standard deviations, indicating stable growth conditions. Conversely, in the T5 zone, the standard deviations of these indices, particularly NDVI and NIR, increase significantly, reflecting the adverse effects of water stress on vegetation growth.

This analysis underscores the crucial role of canopy temperature and spectral reflectance in monitoring water stress in tea trees and provides valuable insights for understanding the physiological responses of tea trees to varying moisture levels.

Model prediction and verification

In this study, multiple machine learning regression models were utilized to predict the canopy temperature of tea trees, including SVR, RF, KNR, and BP neural network. Table 2 presents the error analysis results for the training and validation datasets across these models. Among the models, the RF model demonstrated the best performance, achieving R^2 values of 0.869 and 0.802 for the

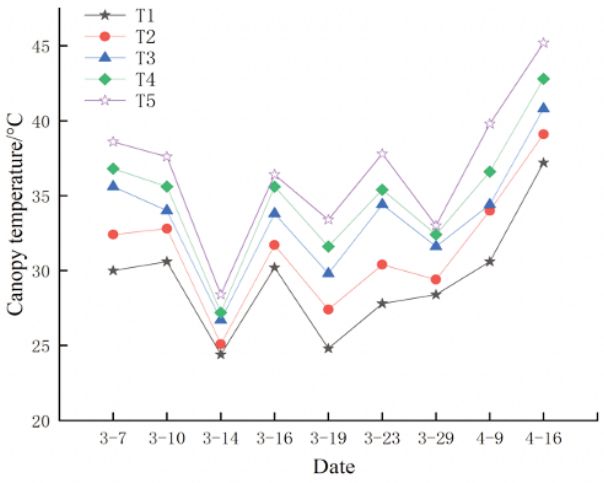

Figure 7. Variation in canopy temperature across different dates under five water treatment conditions (T1-T5). T1 represents sufficient irrigation, while T5 indicates extreme water stress. As water stress intensifies, the fluctuation in canopy temperature becomes more pronounced, with T5 exhibiting the highest temperature and fluctuation range. These changes reflect the impact of transpiration reduction and stomatal closure under water stress.

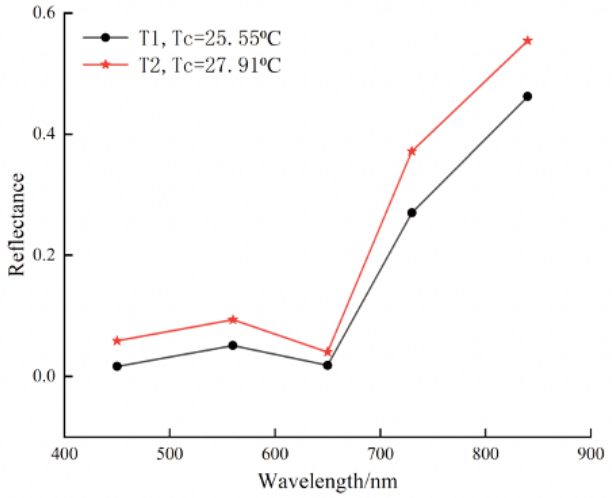

Figure 8. Spectral reflectance of tea leaves under two conditions: full irrigation (T1, T_c=25.55°C) and mild water stress (T2, T_c=7.91°C). Reflectance in the red-edge (730 nm) and near-infrared (840 nm) bands increases significantly with rising canopy temperature, indicating physiological changes in leaf structure and photosynthetic activity under water stress. Reflectance in the blue (450 nm) and green (560 nm) bands remains relatively stable.

Table 1. Vegetation index of tea leaves under different water conditions.

Spring tea period	Data characteristic	Vegetation index				
		NIR	NDVI	DVI	RDVI	OSAVI
T1	Maximum value	0.5	0.95	0.49	0.68	0.84
	Minimum value	0.42	0.86	0.40	0.60	0.74
	Mean value	0.46	0.92	0.44	0.64	0.80
	Standard deviation	0.0246	0.0216	0.0264	0.0242	0.0231
T2	Maximum value	0.59	0.93	0.55	0.72	0.85
	Minimum value	0.45	0.82	0.41	0.58	0.72
	Mean value	0.55	0.86	0.51	0.67	0.79
	Standard deviation	0.0357	0.0307	0.0360	0.0312	0.0302

NIR, near-infrared; NDVI, normalized difference vegetation index; DVI, difference vegetation index; RDVI, renormalized difference vegetation index; OSAVI, optimized soil-adjusted vegetation index.

Table 2. Performance metrics of machine learning models for canopy temperature prediction. This table summarizes the performance of four machine learning models for predicting the canopy temperature of tea trees.

Model	Modeling set			Validation set		
	RMSE/°C	MAE/°C	R^2	RMSE/°C	MAE/°C	R^2
SVR	1.256	0.952	0.825	1.299	1.013	0.774
RF	0.985	0.777	0.869	1.473	1.095	0.802
KNR	1.12	0.819	0.85	1.326	1.084	0.783
BP	1.397	1.08	0.761	1.61	1.239	0.723

SVR, support vector regression; RF, random forest; KNR, K-nearest neighbors; BP, backpropagation.

training and validation datasets, respectively. The RMSE values were 0.985°C for the training set and 1.473°C for the validation set, while the MAE values were 0.777°C and 1.095°C. These results indicate that the RF model has strong generalization capability and provides accurate predictions of canopy temperature. In contrast, the BP neural network exhibited the weakest performance on the validation set, with an R^2 value of only 0.723. By integrating the predicted canopy temperature with the canopy-air temperature difference limits determined by the OPTICS clustering algorithm, the CWSI was calculated. Figure 9 compares the predicted and observed CWSI values, showing a correlation coefficient (R^2=0.73) . This result demonstrates that CWSI prediction based on the RF model can effectively and rapidly diagnose the water stress status of tea trees, making it a practical tool for irrigation management. However, under conditions of low water stress, some prediction errors remain. Future work should focus on optimizing model parameters and incorporating additional environmental variables to further enhance prediction accuracy.

Discussion

This study developed a model to calculate the CWSI for tea trees by integrating various water treatments, the OPTICS clustering algorithm, and UAV-based multispectral image analysis. The model's effectiveness in monitoring tea tree water status was successfully validated. The results indicate a strong correlation between the canopy-air temperature difference and soil moisture content. The OPTICS clustering algorithm effectively extracted the upper and lower limits of the canopy-air temperature difference based on soil moisture data. Compared to traditional empirical models, the limits identified using the OPTICS method were more stable, achieving a coefficient of determination (R^2) of 0.74. This confirms the feasibility of applying this method to monitor tea tree water stress. The method's primary advantage lies in its reliance on stable soil moisture changes, minimizing interference from meterological factors such as temperature, humidity, and light intensity, and providing a more reliable water stress assessment.

The study also revealed significant differences in canopy temperature and spectral reflectance under various water conditions. Under low soil moisture conditions, the canopy-air temperature difference exhibited a wider variation range, with greater fluctuations in canopy temperature and a noticeable increase in reflectance within the red-edge (730 nm) and near-infrared (840 nm) bands. To statistically validate the observed differences in spectral reflectance under varying water treatments, a one-way ANOVA was conducted on the 730 nm (red-edge) and 840 nm (near-infrared) bands across the five treatment groups (T1-T5). The results showed significant differences for both wavelengths (730 nm: F = 21.68, p<0.001; 840 nm: F = 46.10, p<0.001), indicating that canopy reflectance increased significantly with water stress severity. As illustrated in Figure 10, the distribution of reflectance values clearly shifts upward from T1 to T5 in both spectral bands, with the most substantial elevation observed in the NIR region. These findings support the physiological rationale for using red-edge and near-infrared wavelengths to monitor water stress in tea canopies. These findings suggest that while canopy temperature is strongly influenced by soil moisture, it may also be affected by other environmental factors, such as ambient temperature and light intensity. For tea trees under full irrigation, the canopy temperature showed minimal variation, and the vegetation indices displayed smaller standard deviations, indicating stable growth conditions. In contrast, water stress conditions led to greater fluctuations in both canopy temperature and spectral reflectance. These results provide valuable insights into diagnosing tea tree water stress and optimizing irrigation management practices. Additionally, this study verified the potential of UAV multispectral images for predicting the canopy temperature of tea trees. By analyzing the correlation between vegetation indices and canopy temperature, the R-based prediction model outperformed other machine learning models on both the training and validation datasets, demonstrating high prediction accuracy and robust generalization ability. This spectral data-based prediction method

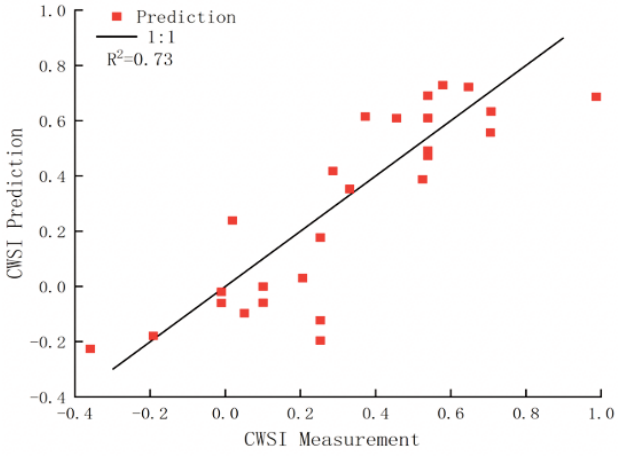

Figure 9. Comparison between predicted and measured CWSI values, calculated using the RF model, and the observed CWSI measurements. The black solid line represents the ideal 1:1 relationship, while the red squares depict the predicted data points.

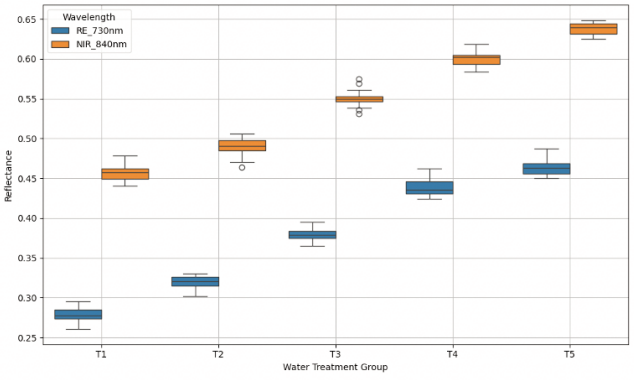

Figure 10. Variation in spectral reflectance at two key wavelengths -red-edge (730 nm) and near-infrared (840 nm)- under five water treatment conditions (T1-T5). T1 represents sufficient irrigation, while T5 indicates extreme water stress. As water stress intensifies, reflectance values at both wavelengths increase progressively, with T5 showing the highest levels. These changes reflect reduced chlorophyll absorption and increased leaf scattering associated with stomatal closure and altered canopy structure under water-limited conditions.

OPEN ACCESS

enables the rapid acquisition of canopy temperature information across large-scale tea plantations, facilitating real-time monitoring of tea tree water stress. Although this study focused on a relatively short data collection window during the spring tea season (March to April), this period represents the most critical growth stage for tea trees, when leaf quality and yield potential are at their peak. Spring tea is highly valued for its superior flavor and chemical composition, making this season especially relevant for precision irrigation and water stress assessment. Nevertheless, seasonal variations in environmental conditions -such as temperature, humidity, and solar radiation- may influence the physiological response of tea trees and affect the stability of model performance. Future research should therefore incorporate multi-season or year-round data collection to validate and improve the generalizability of the proposed models across diverse phenological stages and climatic conditions.

Despite the significant advantages demonstrated by the OPTICS clustering algorithm and UAV spectral analysis in monitoring tea tree water stress, certain limitations remain. For instance, data consistency may be influenced by varying weather conditions. Future studies are recommended to increase control over experimental conditions or conduct experiments in greenhouse environments to minimize interference from external factors. Furthermore, integrating additional data, such as leaf stomatal conductance and physiological response metrics, could help construct a more comprehensive water stress assessment model.

In summary, this study proposes a novel approach to tea tree water stress monitoring by combining the OPTICS clustering algorithm and UAV-based multispectral analysis. The method achieves accurate canopy temperature prediction and efficient CWSI calculation, making it both theoretically innovative and practically applicable. This approach offers valuable technical support for precise irrigation management in tea tree cultivation.

Conclusions

This study investigated the water stress status of tea trees during the spring tea harvest period by utilizing UAV multispectral imagery combined with soil moisture content and canopy temperature data collected under varying water treatments. By establishing machine learning models and integrating the OPTICS clustering algorithm, the following key findings were obtained:

1. Determination of canopy-air temperature difference limits: Using soil moisture content and canopy-air temperature difference as variables, the OPTICS clustering algorithm successfully identified the upper and lower limits of the canopy-air temperature difference for tea trees. Compared to traditional empirical models for CWSI calculation, the lower limit determined by the OPTICS method demonstrated higher accuracy and stability, with a coefficient of determination (R^2=0.74), highlighting its effectiveness in water stress monitoring.
2. Canopy temperature prediction model: For predicting canopy temperature using vegetation index inversion, the RF model achieved the best performance, with R^2>0.8 for both the training and validation datasets. The RF model also recorded a validation set RMSE of 1.473°C, demonstrating high prediction accuracy and strong generalization ability. In contrast, the BP neural network yielded the poorest results, underscoring its limitations in this application.
3. Rapid CWSI calculation: By integrating the OPTICS clustering algorithm with the RF-based prediction model, the CWSI was calculated rapidly, achieving an R^2=0.73. This method proved to be effective for monitoring the water stress status of tea trees and offers practical technical support for precision irrigation management.

References

Awais, M., Li, W., Cheema, M.J.M., Zaman, Q.U., Shaheen, A., Aslam, B., et al. 2023. UAV-based remote sensing in plant stress imagine using high-resolution thermal sensor for digital agriculture practices: a meta-review. Int. J. Environ. Sci. Technol. 20:1135–1152.

Bhandari, S., Raheja, A., Chaichi, M.R., Green, R.L., Do, D., Pham, F.H., et al. 2018. Lessons learned from UAV-based remote sensing for precision agriculture. Proc. Int. Conf. on Unmanned Aircraft Systems (ICUAS), Dallas, pp. 458-467.

Cheng, Q., Ding, F., Xu, H., Guo, S., Li, Z., Chen, Z. 2024. Quantifying corn LAI using machine learning and UAV multispectral imaging. Precision Agric. 25:1777-1799.

de Castro, A.I., Shi, Y., Maja, J.M., Peña, J.M. 2021. UAVs for vegetation monitoring: Overview and recent scientific contributions. Remote Sens. 13:2139.

Deng, L., Mao, Z., Li, X., Hu, Z., Duan, F., Yan, Y. 2018. UAV-based multispectral remote sensing for precision agriculture: A comparison between different cameras. ISPRS J. Photogramm. Remote Sens. 146:124–136.

Feroz, S., Abu Dabous, S. 2021. UAV-based remote sensing applications for bridge condition assessment. Remote Sens. 13:1809.

Ge, X., Wang, J., Ding, J., Cao, X., Zhang, Z., Liu, J., Li, X. 2019. Combining UAV-based hyperspectral imagery and machine learning algorithms for soil moisture content monitoring. PeerJ 7:e6926.

Guofeng, Y., Yong, H.E., Xuping, F., Xiyao, L.I., Jinnuo, Z., Zeyu, Y.U. 2022. Methods and new research progress of remote sensing monitoring of crop disease and pest stress using unmanned aerial vehicle. Smart Agriculture 4:1.

Guptha, G.C., Swain, S., Al-Ansari, N., Taloor, A.K., Dayal, D. 2021. Evaluation of an urban drainage system and its resilience using remote sensing and GIS. Remote Sens. Appl. 23:100601.

Harle, S., Bhagat, A., Dash, A.K. 2024. Remote sensing revolution: mapping land productivity and vegetation trends with unmanned aerial vehicles (UAVs). Curr. Appl. Mater. 03:e070224226752.

Huang, G., Li, Z., Li, X., Liang, S., Yang, K., Wang, D., Zhang, Y. 2019. Estimating surface solar irradiance from satellites: Past, present, and future perspectives. Remote Sens. Environ. 233:111371.

Idso, S.B., Jackson, R.D., Pinter, P.J., Reginato, R.J., Hatfield, J.L. 1981. Normalizing the stress-degree-day parameter for environmental variability. Agric. Meteorol. 24:45-55.

Jeong, S., Ko, J., Kim, M., Kim, J. 2016. Construction of an unmanned aerial vehicle remote sensing system for crop monitoring. J. Appl. Remote Sens. 10:026027.

Khanal, S., Kc, K., Fulton, J.P., Shearer, S., Ozkan, E. 2020. Remote sensing in agriculture - accomplishments, limitations, and opportunities. Remote Sens. 12:3783.

Kouadio, L., El Jarroudi, M., Belabess, Z., Laasli, S.-E., Roni, M.Z.K., Amine, I.D.I., et al. 2023. A review on UAV-based applications for plant disease detection and monitoring. Remote Sens. 15:4273.

Kumar Jha, S., Ramatshaba, T.S., Wang, G., Liang, Y., Liu, H., Gao, Y., Duan, A. 2019. Response of growth, yield and water use efficiency of winter wheat to different irrigation methods and scheduling in North China Plain. Agric. Water Manag. 217:292-302.

Li, X., Hu, T., Gong, P., Du, S., Chen, B., Li, X., Dai, Q. 2021. Mapping essential urban land use categories in Beijing with a fast area of interest (AOI)-based method. Remote Sens. 13:477.

Liu, X., Peng, Y., Yang, Q., Wang, X., Cui, N. 2021. Determining optimal deficit irrigation and fertilization to increase mango yield, quality, and WUE in a dry hot environment based on TOPSIS. Agric. Water Manag. 245:106650.

Maes, W.H., Steppe, K. 2019. Perspectives for remote sensing with unmanned aerial vehicles in precision agriculture. Trends Plant Sci. 24:152-64.

Maimaitijiang, M., Sagan, V., Sidike, P., Daloye, A.M., Erkbol, H., Fritschi, F.B. 2020. Crop monitoring using satellite/UAV data fusion and machine learning. Remote Sens. 12:1357.

Ndlovu, H.S., Odindi, J., Sibanda, M., Mutanga, O., Clulow, A., Chimonyo, V.G., Mabhaudhi, T. 2021. A comparative estimation of maize leaf water content using machine learning techniques and unmanned aerial vehicle (UAV)-based proximal and remotely sensed data. Remote Sens. 13:4091.

Osco, L.P., Marcato Junior, J., Marques Ramos, A.P., de Castro Jorge, L.A., Fatholahi, S.N., de Andrade Silva, J., et al. 2021. A review on deep learning in UAV remote sensing. Int. J. Appl. Earth Observ. Geoinform. 102:102456.

Pipatsitee, P., Tisarum, R., Taota, K., Samphumphuang, T., Eiumnoh, A., Singh, H.P., Cha-Um, S., 2023. Effectiveness of vegetation indices and UAV-multispectral imageries in assessing the response of hybrid maize (Zea mays L.) to water deficit stress under field environment. Environ. Monit. Assess. 195:128.

Romero, M., Luo, Y., Su, B., Fuentes, S., 2018. Vineyard water status estimation using multispectral imagery from an UAV platform and machine learning algorithms for irrigation scheduling management. Comput. Electron. Agric. 147:109-117.

Shi, Y., Gao, Y., Wang, Y., Luo, D., Chen, S., Ding, Z., Fan, K., 2022. Using unmanned aerial vehicle-based multispectral image data to monitor the growth of intercropping crops in tea plantation. Front. Plant Sci. 13:820585.

Su, J., Coombes, M., Liu, C., Zhu, Y., Song, X., Fang, S., et al. 2020. Machine learning-based crop drought mapping system by UAV remote sensing RGB imagery. Unmanned Syst. 08:71-83.

Tsouros, D.C., Bibi, S., Sarigiannidis, P.G., 2019. A review on UAV-based applications for precision agriculture. Information 10:349.

Wang, P., Luo, X., Zhou, Z., Zang, Y., Hu, L., 2014. Key technology for remote sensing information acquisitionbased on micro UAV. T. CSAE 30:1-12.

Wang, Q., Cheng, M., Xiao, X., Yuan, H., Zhu, J., Fan, C., Zhang, J., 2021. An image segmentation method based on deep learning for damage assessment of the invasive weed Solanum rostratum Dunal. Comput. Electron. Agric. 188:106320.

Wu, W., Mao, W., 2022. An efficient and scalable algorithm to mine functional dependencies from distributed big data. Sensors 22:3856.

Yin, N., Liu, R., Zeng, B., Liu, N., 2019. A review: UAV-based remote sensing. IOP Conf. Ser. Mater. Sci. Eng. 490:062014.

Yubin, L., Xiaoling, D., Guoliang, Z., 2019. Advances in diagnosis of crop diseases, pests and weeds by UAV remote sensing. Smart Agriculture 1:1.

Zhang, H., Wang, L., Tian, T., Yin, J., 2021. A review of unmanned aerial vehicle low-altitude remote sensing (UAV-LARS) use in agricultural monitoring in China. Remote Sens. 13:1221.

Zou, X., Jin, J., Mõttus, M., 2023. Potential of satellite spectral resolution vegetation indices for estimation of canopy chlorophyll content of field crops: mitigating effects of leaf angle distribution. Remote Sens. 15:1234.

Received: 24 February 2025; Accepted: 9 September 2025.

Contributions: all authors made a substantive intellectual contribution, read and approved the final version of the manuscript and agreed to be accountable for all aspects of the work.

Conflict of interest: the authors declare that no known competing financial interests or personal relationships that could have appeared to influence the work reported in this paper.

Funding: this research was funded by the Education Ministry's Collaborative Education Program with Industry (No. 230702595161723). It was also partly supported by the Guangdong Science and Technology Innovation Cultivation Special Fund Project for College Students ("Climbing Program" Special Fund), China (No. pdjh2023a0074); the Undergraduate Innovation and Entrepreneurship Training Program (NO. 2023105641146).

Publisher's note: all claims expressed in this article are solely those of the authors and do not necessarily represent those of their affiliated organizations, or those of the publisher, the editors and the reviewers. Any product that may be evaluated in this article or claim that may be made by its manufacturer is not guaranteed or endorsed by the publisher.

This work is licensed under a Creative Commons Attribution-NonCommercial 4.0 International License (CC BY-NC 4.0).